# Black Start of Coastline Power Networks From Grid-Forming Ship-to-Grid Services

Sobhan Badakhshan, *Graduate Student Member, IEEE*, Jubeyer Rahman, *Graduate Student Member, IEEE*, and Jie Zhang, *Senior Member, IEEE*

***Abstract*—The expansion of electric ships in the transportation sector, along with environmental advantages, has the potential to enhance the resilience and stability of coastline power grids during blackouts or emergencies through ship-to-grid technology. The power grids located in remote coastal and island communities often face high energy costs and are more vulnerable to blackouts due to their increased risk of natural disasters. Ship-to-grid technology offers an innovative localized solution that enables onshore utilities to avoid the need for installing excessive on-land energy storage capacity to enhance stability and resiliency in the coastline power grid. Electric ships can provide a flexible source to restart power to critical facilities such as hospitals and communication networks. In this paper, a comprehensive scheme for integrating ships into the grid system is proposed, which involves a grid-forming control approach through a DC-link connection. The approach employs a droop-based control strategy, current limiter control, and voltage source grid interface to regulate both voltage and frequency at various stages of the coastline power network restoration. The approach is verified using a 4-zone shipboard power system with grid-forming DC-link connection, for black start of a modified IEEE 30-bus test system during a multi-step black start and re-energization process.**

***Index Terms*—Shipboard power system, ship-to-grid, ship-to-shore, DC-link, grid-forming, black start.**

## I. Introduction

ELECTRICAL grids at coastline areas are predominantly vulnerable to natural disasters, which could result in cascading failures and potential blackouts. In recent years, the frequency of extreme weather event-driven large-scale power outages has gone up significantly [1], [2], [3]. There have been incidents of extreme weather events causing widespread power interrupts that lasted up to weeks, and few of them resulted in blackouts [4], [5]. To combat the catastrophic impact of natural disasters, it is crucial to enhance the resilience of the power grid, thereby reducing the duration of grid outages and improving network restoration. Mobile emergency resources could play a pivotal role in building a resilient power grid with its multitude of benefits in the reduction of the recovery time [6]. The integration of marine energy vessels into the onshore power grid is a promising and growing technology [7], driven by the emergence of new generations of electric ships and ferries with higher capacity. For example, an electric car may have a battery size of 40-100 kWh, while an electric ferry or cruise ship may have a battery size in the range of several MWh (megawatt-hours) [8].

Integration of ships into the grid has the potential to provide environmental and economic benefits but requires careful planning and investment in infrastructure and technology to be successful.Ensuring the safety and reliability of both grids poses a significant challenge, as connecting ships to the grid can potentially create issues with voltage and frequency stability. For example, analyses [9], [10] have been conducted to assess the potential impact of the loads from large cargo or cruise ships on the voltage stability and reliability of the offboard utility grid, to identify any underlying problems that could potentially degrade the grid's performance. The shipboard power system (SPS) can be considered a microgrid that operates in islanded mode, offering a flexible, efficient, environmentally friendly, reliable, and cost-effective solution for powering loads in shore power grids and ship-to-grid applications. It can supply power to shore-based loads, other ships, and offshore installations while reducing losses during transmission and distribution. SPS can provide a reliable power source, which can help to reduce the need for installing backup generators and other associated costs. The Power Management System (PMS) on ships is responsible for controlling generators to ensure the availability of electrical power and prevent blackouts. By connecting the generator sets on an SPS to a de-energized bus, they can provide various services to the onshore grid, including operating at a reduced load level when disconnected from the grid, maintaining frequency when picking up a block of load, dynamic off-line testing of the governor system, and maintaining voltage by varying voltage setting while on load and synchronized to the system.

Despite the significant amount of literature on the study of shore-to-ship and cold ironing, there are few studies in the literature on ship-to-shore interconnection. Ship-to-grid studies can be classified into two main categories: dynamic and real-time modeling, and long-term planning and operation. For example, [11] has investigated the use

Manuscript received 8 February 2023; revised 7 May 2023; accepted 18 June 2023. Date of publication 29 June 2023; date of current version 21 February 2024. This work was supported in part by the Department of the Navy, Office of Naval Research (ONR) under Award N00014-20-1-2795, and in part by the U.S. Department of Energy under Award DE-NE0009296. Paper no. TSG-00181-2023. *(Corresponding author: Jie Zhang.)*

Sobhan Badakhshan and Jubeyer Rahman are with the Department of Electrical and Computer Engineering, The University of Texas at Dallas, Richardson, TX 75080 USA.

Jie Zhang is with the Department of Mechanical Engineering and the Department of Electrical and Computer Engineering, The University of Texas at Dallas, Richardson, TX 75080 USA (e-mail: jiezhang@utdallas.edu).

Color versions of one or more figures in this article are available at https://doi.org/10.1109/TSG.2023.3290560.

Digital Object Identifier 10.1109/TSG.2023.3290560

of SPS as an emergency mobile energy system to support the power grid during disruptive events and improve the resiliency of distribution networks through ship-to-grid capability. Vlachokostas et al. [7] explored the ship's potential to provide grid ancillary services (such as frequency regulation and load balancing) to an onshore power grid. The ship-to-grid connections could be developed in a long-term strategic plan for optimal ship energy management. For instance, Wen et al. [12] have studied the impact of electricity prices on the electric ferry interconnection, by considering the ship routing. Zhou et al. [13] proposed an energy cooperation coalition scheme that comprises multi-island microgrids, and all-electric ships are used for energy sharing.

The integration of electric ships into the coastline power grid requires a careful assessment of both the hardware and software on both the SPS and onshore sides. To address this issue, a dedicated shore station should be employed to connect the ship-to-grid, with the aim of enhancing the voltage and frequency stability of both the SPS and the onshore grid. This approach may even offer assistance in maintaining the stability and reliability of the local grid. Some possible ship-to-grid interconnection strategies have been discussed in [14], [15]. While the process of ship-to-grid connection has been evaluated in previous work, there has been a lack of comprehensive investigation into the potential to offer different types of grid services. The concentrated connection of several electric ships can potentially cause stress on the local power grid, resulting in voltage fluctuations and potential blackouts. DC-Link technology combines power electronics and fast switching control to offer a high degree of control flexibility. It can react quickly to load changes, making it ideal for applications that require rapid adjustments to voltage or current output. DC-Link technology also includes higher efficiency and power quality, and ensures that the ship's power system is compatible with the onshore power grid and that the transfer of power does not cause any electrical or mechanical damage to either system [16]. The conventional schemes for the dc-link are not able to function during the black start of a grid when there is no measured voltage or frequency at the connection point. Therefore, a grid-forming (GFM) control scheme is developed in this paper to dynamically control dc-link systems and enable ship-to-grid black start services. A significant amount of work has been performed in grid-forming technologies. For example, when HVDC transmission systems are controlled by grid-forming systems, a stability analysis of power systems has been performed by a center-of-inertia formulation for a multi-grid-forming inverter-based power system [17], [18]. Rokrok et al. [19] have introduced a droop-based grid-forming control strategy by including virtual inertia emulation for active power regulation and frequency support. The grid integration of renewable resources by using grid-forming inverters has been extensively studied [20]. Detailed comparisons between grid-following and grid-forming inverters have also been conducted to explore the potential of grid-forming inverter technologies in support of resiliency and stability of power systems [21], [22], [23]. Although grid-forming control has been studied in the literature, its application for grid integration of electric marine vessels to improve resiliency and enable black starts of shoreline grids is still a novel approach.

The purpose of this study is to evaluate the resilience and stability enhancement of the grid by the integration of electric ships. The motivation for this research is to explore the potential applications of electric ships beyond transportation. Electric ships can serve as mobile energy storage systems that can be integrated into a microgrid or a large-scale grid to enhance its resilience and stability. Black-start operations can be challenging in remote or islanded locations, and electric ships can provide a reliable and flexible source of power to restart the coastline grid. The noteworthy contributions of the paper are highlighted as follows:

1) Comprehensive black start scheme: This paper proposes a comprehensive black start scheme for terrestrial networks, combining SPS and DC-Link technology. This integration is expected to enhance the resilience and reliability of power systems during blackouts and other disturbances.
2) Droop-based control loop: This paper proposes a grid-forming DC-link control scheme that can maintain voltage and frequency stability in the coastline power grid, enabling black start services even when no measurements are available in the coastal electric grid. The droop-based control loop has been included to provide support for voltage and frequency stability.
3) Current limit issue: In order to effectively handle the inrush current during a black start, the current limiter controls only one component of the current, while the maximum value of the second component is calculated based on both the maximum allowable current magnitude of the converter and the maximum value of the other component of the current in the $d-q$ framework. To prevent excessive current at the start of a black start, in addition to the current limiter control block, a voltage controller in the grid-forming dc-link loop is developed to gradually increase the voltage by ramping references up and regulating the voltage output of the inverter to match the voltage of the inverter system with grid.
4) Dynamic models of various components: This paper provides insights into the dynamic behavior and stability of ship-to-grid interconnection by grid-forming control of the DC-link, using the dynamic models of various components and systems of SPS and shore grid. This approach has not been explicitly explored in existing studies.

The rest of the paper is organized as follows. The SPS dynamic model for ship-to-grid connection is present in Section II. The grid-forming DC-link for the black start of the grid is described in Section III. Section IV presents the simulation framework and cases to demonstrate the effectiveness of the proposed control, followed by the conclusion in Section V.

## II. Connecting SPS to Coastline Electric Grid

Electric ships and SPSs provide an effective solution for the black start of a coastline power grid, and they are mobile

power sources that can operate independently from the grid and be deployed rapidly to the impacted area, providing power to essential facilities and infrastructure within a matter of hours. These systems are designed to operate independently of the primary power grid, making them well-suited for use in black start procedures and enhancing the resilience of a coastline power grid. The SPS could be considered as a microgrid on the water with distributed resources onboard, interconnected loads within a specified boundary, and operating in both island and grid-connected modes. Similar to a microgrid, there are 1–3 primary generators and one smaller emergency backup generator on the ship as a common practice. The power rating of each of the main generators is typically sufficient to feed a sizable portion of the vessel's electrical load.

Ship-to-grid or ship-to-shore poses both challenges and opportunities for electric utilities. For example, ship-to-grid could provide services to the main grid during demand spikes or power outages. For grid operators, electric ships could contribute as valuable flexible backup energy systems, which potentially help the utility to avoid unnecessary energy storage capacity investments for resiliency enhancement of the coastline power grid. Different types of electric ships could be leveraged for ship-to-grid connections, such as:

*1) Diesel-Electric Systems:* SPSs typically use diesel generators or gas turbines to generate electricity, which can be used to power the ship and its onboard systems, as well as to export power to other locations. These systems are mostly found in large ocean-going container ships. The generator system consists of an alternator and a driver for the alternator which can be a steam-driven or diesel-driven engine. The generator often works on its own and is able to respond to the abrupt connection of motors and large loads. It can handle system load swings and unusual operational requirements.

*2) Electric Ship Fleet:* Electrification of ships is developing rapidly, which could replace diesel power units and offer a low-carbon solution. While the electric vessel market is nascent, in the near future, a fleet of electric ships could be utilized to provide grid services.

*3) Nuclear-Powered Ships (NPS):* Nuclear power is particularly suitable for ships that need to be at sea for a long period of time without refueling. To increase the flexibility and efficiency of NPS during the berthing period, ship-to-grid interconnection could be the best solution to leverage the generated power by the nuclear reactors on NPS.

In this study, gas turbine generators are used as the main generators for the SPS to ensure that power can be restored quickly. Gas turbine generators offer numerous advantages in marine applications, including a high power-to-weight ratio, suitability for use in situations where space and weight are only premium, rapid response times, improved maneuverability of electric motor adjustable speed drives, and reduced noise and vibration. Moreover, the new generation of hybrid AC-DC ships can operate at higher frequencies, enabling greater control of the system with more compact and lighter components, leading to improved efficiency [24].

The selected test SPS layout is illustrated in Fig. 1, including a main generator as the primary source of electricity and

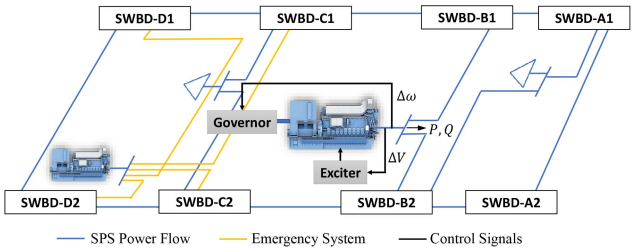


Fig. 1. The layout of shipboard power system generators.

an emergency backup generator, which is smaller, and is supposed to be called on in case of failure and emergencies. The backup generator is located in a separate compartment from the main generator. The dynamic model of each synchronous generator includes three components which are the GENROU for the generator machine model, the GGOV1 for the turbine governor model, and the AC8B for the exciter model to control the automatic voltage regulator system of the generator. The SPS is comprised of four zones: A, B, C, and D. The term SWBD-D1 stands for switchboard distribution at zone D. Each zone has two switchboards, with one located on the port side labeled as 1 and the other on the starboard side labeled as 2.

The total onboard active power loads are shared by the set of synchronized generators as per the frequency control strategy. Each speed governor is responsible to participate in the concerted frequency response scheme of the SPS. The actual load interchange can happen based on the mission priority.

## III. Grid-forming Control for the Black Start

The black start of the remote islands and coastline grids can be different from other grids due to several factors, such as the geographical and topographical features, and the location and limit of power generation facilities. Coastal areas are often subject to harsh weather conditions, what makes matters worse is that these grids often have limited interconnections with other power networks, which makes them more isolated and vulnerable to power outages compared to interconnected grids. For the ship-to-shore and shore-to-ship connections, several onshore schemes have been developed for diverse applications such as onboard battery charging and cold-ironing processes [25]. The developed models could be modified for a stable ship-to-grid connection by leveraging the grid-forming control DC-link scheme, enabling the system to regulate both voltage and frequency.

### A. Droop-Based Grid Forming Control

To black-start the coastal power grid using the SPS, the DC-link inverter should be operated in grid-forming mode, which functions as a voltage source to simulate the inertia of a synchronous machine.

The difference between grid-forming and grid-following converter systems in the operating mode is illustrated in Fig. 2. Fig. 2(a) shows the grid-following vector control. The terminal voltage $V_t$ is created by the rest of the grid (step 1) in the conventional grid-following inverter systems and finally, the source voltage $E$ (step 3) is calculated by the inner control

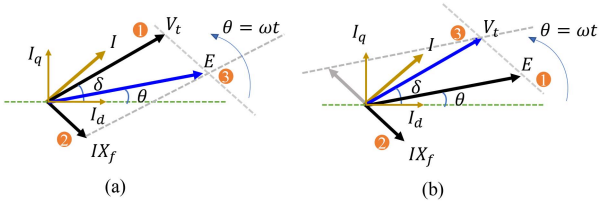


Fig. 2. Phasor diagram of the inverter as a voltage source in (a) grid-following and (b) grid-forming mode of operation.

loop according to Eq. (1). However, in the grid-forming mode of operation, $V_t$ is not available during the black start. Thus, as shown in Fig. 2(b), the control system should create the source voltage of $E\angle\theta$. When it is connected to the grid (step 1), the current injection causes the voltage loss $IX_f$. Finally, in step 3, the resultant vector $V_t$ is calculated by Eq. (2), which is an independent voltage at any condition in the rest of the grid, thereby verifying the role as a voltage source.

$$E\angle\theta = V_t\angle\delta + IX_f \tag{1}$$

$$E\angle\theta - IX_f = V_t\angle\delta \tag{2}$$

The droop-based grid-forming control method is a commonly used technique in islanded or standalone power systems to ensure stable voltage and frequency. This approach involves two primary control loops: (i) an active power-frequency loop that addresses frequency deviation and generates a reference angle, and (ii) a reactive power-Voltage loop that regulates voltage by monitoring reactive power. The equivalent circuit of the inverter system is modeled as a voltage source with amplitude $E$ and phase angle $\delta$. The active and reactive power of the inverter can be calculated as follows:

$$P = \frac{VE}{Z}cos(\theta - \delta) - \frac{V^2}{Z}cos(\theta) \tag{3}$$

$$Q = \frac{VE}{Z}sin(\theta - \delta) - \frac{V^2}{Z}sin(\theta) \tag{4}$$

The assumption that the equivalent connection impedance is inductive is well-founded due to the significant inductive components present in high-voltage or medium-voltage systems, thus $\theta$ is set to be 90 deg. The grid-forming control blocks are responsible for holding the phase angle and voltage magnitude reference constant. As illustrated in Fig. 3, the droop-based control layer is embedded in the grid-forming controller to regulate voltage and frequency to their reference set points. The droop control has been used as a base method for various purposes such as improving transient performance, coordinating different types of inverters, ensuring system reliability and security, and designing control strategies for various system constraints and objectives in different studies [26], [27], [28]. To address several issues related to the black start process, a droop-based control is designed to create and control voltage and frequency references at the connection point, which can be crucial in situations where quick and reliable power restoration is required.

To mitigate deviations in frequency and voltage from the set point value, the droop-based controller is formulated as

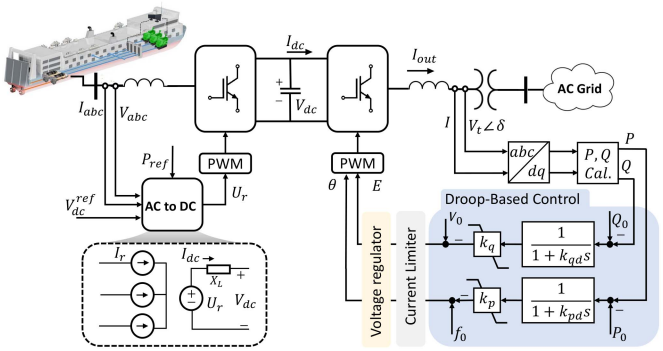


Fig. 3. Droop-based scheme of grid-forming control applied to the ship-to-grid DC-link.

follows.

$$\theta = \int 2\pi(f_0 - f)dt \tag{5}$$

$$f = f_0 - k_p(P - P_0) - k_{pd}\frac{dP}{dt} \tag{6}$$

$$E = E_0 - k_q(Q - Q_0) - k_{qd}\frac{dQ}{dt} \tag{7}$$

where $f$ and $E$ are the grid frequency and voltage determined from the droop control scheme, and $f_0$ and $E_0$ are the reference set points of frequency and voltage, respectively. $k_p$, $k_{pd}$, $k_q$, and $k_{qd}$ are the proportional and integral gains of a PI controller, which are tuned as per the grid control requirements. Equation (5) shows that the angle $\theta$ between the voltage and current phasors is proportional to the frequency deviation from the set point. Equations (6) and (7) show that the actual frequency and voltage are determined by the difference between the set point value and a weighted sum of the real and reactive power deviation, along with their respective derivatives, to respond any change that may occur.

Therefore, by including the dynamic model of the DC voltage, the developed grid-forming scheme is evaluated from the perspective of black start and synchronization. As depicted in Fig. 3, the proposed controller utilizes the terminal voltage measurement $V_t$. If no voltage is detected, the droop-based control loop creates frequency and voltage references to the system. The terminal voltage $V_t$ is created based on the load current measurement from the connected system. Since the medium voltage AC SPS supplies the DC power, the DC bus voltage at the inverter end does not remain constant. To address this issue, the onboard gas turbine generator could control the DC-link capacitor voltage.

According to the AC to DC controller shown in Fig. 3, the DC side is represented by a controlled voltage source, and $I_r$ as a reference current of the AC side would be calculated by $U_r$ and $I_{dc}$ in the converter model.

### B. Voltage Source Modeling by Current Limit Control

When black-starting a coastline grid using an SPS integration, it is crucial to take into account the inrush current, voltage stability, frequency regulation, and synchronization between different generation resources and demand. During the initial energization of the grid, the control strategy must

**Algorithm 1** Current Limiter Control

**Require:** $I_{qcmd}$,$I_{max}$,$I_{pcmd}$ are the input current
**Ensure:** $I_p^{min}$,$I_p^{max}$,$I_q^{min}$,$I_q^{max}$ are the output

$I_p^{max} \leftarrow I_{max}$
**if** $|Ipcmd| > Imax$ **then**
  $I_p^{max} = Imax$
**else**
  $I_p^{max} = Ipcmd$
**end if**
$I_q^{max} = \sqrt{Imax^2 - I_p^{max2}}$
$I_q^{min} = -Iqmax$
End

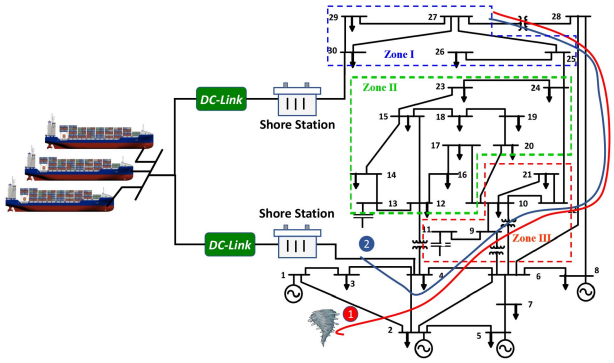


Fig. 4. Modified IEEE 30-bus test system affected by a hurricane disruptive event with two different trajectories.

restrict the inrush current and gradually increase the power output to prevent damage. Furthermore, it is essential to regulate frequency and voltage levels to preserve voltage stability. The frequency must be carefully controlled to prevent damage to connected equipment and ensure a stable power supply. After the black-start process, the control strategy must manage synchronization and ensure a consistent and stable power supply.

In order to effectively handle the inrush current during a black start, the current limiter controls only one component of the current, while the maximum value of the second component is calculated based on both the maximum allowable current magnitude of the converter, $I_{max}$, and the maximum value of the other component of the current in the $d-q$ framework. As shown in Algorithm 1, the grid-forming dc-link system in this case considers the $d$ current, which corresponds to active power that is controlled by the maximum allowable current. However, other studies in the literature [29], [30] seek to control both components of the current. The current limiter is used to control the active power ramp rate in response to the current operating situation by limiting the difference between the maximum current limit ($I_p^{max}$) and the commanded current ($I_{pcmd}$). The implementation of the limiter is vital because it prevents sudden and excessive fluctuations in power output. Where $I_p^{max}$, $I_p^{min}$, $I_q^{max}$, and $I_q^{max}$ are the maximum and minimum allowable current for $d$ and $q$ component, respectively. Inverter-based systems rely on two key control parameters, namely the maximum d-current and the reactive current limit, to facilitate grid recovery in this scenario. The adopted method in this study considers the maximum acceptable boosting span of rising current and the maximum allowable complex current value to sustain stability [31].

To maintain an effective voltage-supporting function, the inverter should avoid reaching its current limit when the load increases. Additionally, for controlling the active and reactive components of the output current, the real power capability of the DC-link should be able to generate the required real power to meet the load demand, even when the grid is unable to provide the necessary voltage support. The PI controller adjusts the desired reactive and active components of the inverter current ($I_q$ and $I_d$) based on the error and deviation from reference values. If the injected current by the droop-based controller is less than the rated current, the current loop controller adjusts the desired phase and magnitude to the reference values for ac waveform, so the inverter acts as a voltage source. To maintain the constant magnitude of the complex current, the prioritization scheme allows the inverter to supply the demanded $I_d$ while decreasing $I_q$.

## IV. Results and Discussion

This section aims to explore the potential of SPS in aiding energization sequence, load pickup, and grid synchronization, while also providing black start service to the coastline power network. To evaluate the system performance, the impacts on the AC bus voltage, DC-link terminal voltage, and active and reactive power dispatch of the SPS generators, during the black start process are analyzed. The sufficient power capacity for black-starting a coastline microgrid is supplied by three SPSs, with each capable of supplying up to 33 MW. The onboard electrical loads (such as propulsion motors, air conditioning, etc.) are kept off while the ship-to-grid interconnection process is being performed. The coastline power grid is represented by a modified IEEE 30-bus test system, which has two different zones with the voltage levels of 33 kV and 230 kV [32]. The 33 kV zone can be isolated from the 230 kV zone by taking four transformers out of service. A microgrid is formed in the 33 kV network as a case study to demonstrate the black start process.

The test network has a total electrical load of 81 MW. To study the black start process, two cases are considered with different trajectories of the hurricane to traverse the test network, as illustrated in Fig. 4. The red and blue trajectories illustrate the conditions of the grid in two scenarios. The red cut-set in the first scenario involves creating a weak grid with only one generator to evaluate the impact of integrating SPS on the improvement of grid stability. The blue cut-set in the second scenario simulates a blacked-out grid by disconnecting all generating units. Although the two trajectories may appear similar, they represent distinct scenarios due to the presence of a generator. Therefore, the system demand should be taken up by the generators in SPS. The SPS alone should provide suitable conditions for subsequent synchronization of other units to be sequentially connected to the grid. The dynamic simulation of the integrated system is performed by importing the SPS model into PSS/Netomac, and the simulation results are

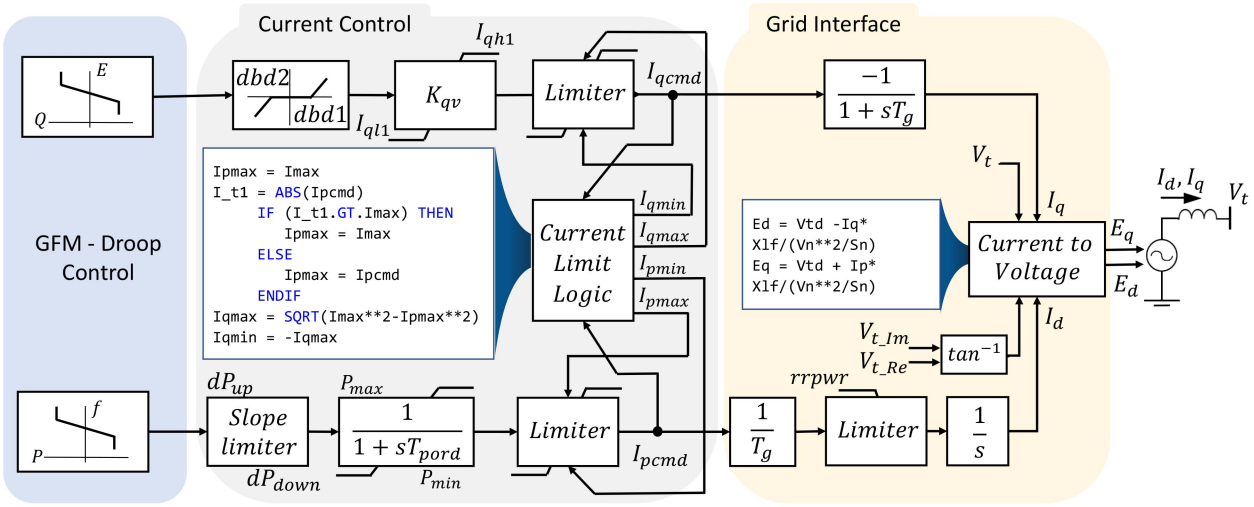


Fig. 5. Dynamic grid interface of the grid-forming control.

also analyzed in the PSS/Netomac workspace. The simulation executed over a period of 10 seconds. To account for different possible scenarios, the study considers and analyzes the following three situations.

*1) Dynamic Modeling of the Grid-Forming DC-Link:* The dynamic model for grid-forming control has been developed on the graphical model builder (GMB) module of PSS/Netomac. Before incorporating the proposed inverter control system model into the power system simulation, it is essential to ensure its accurate development and thorough testing. Once the model is designed and tested, it can be directly integrated as a macro file in the power system study, using the developed grid-forming control model.

The inverter is modeled as a voltage source to supply voltage support to the system. The voltage source is formed by $I_d$ and $I_q$. Both input variables of the model are interpreted as real and imaginary parts of a voltage phasor. The output of the droop-based control system is modulated to the real and imaginary parts of a voltage, to be fed into the voltage source model. Figure 5 illustrates the dynamic grid interface of the grid-forming control. To have a controllable voltage source, the $d-q$ current components in the current limiter are implemented as a controller for the voltage vector.

The modulus of the current vector is shown in the current limit logic block in Fig. 5. The grid interface compares the outputs of the current controllers with the terminal voltage measurement. The $E\angle\theta$ values with $d-q$ voltage components are then modulated as follows:

$$E_d = V_{td} - I_q \frac{X_f}{\frac{V_n^2}{S_n}} \tag{8}$$

$$E_q = V_{tq} + I_p \frac{X_f}{\frac{V_n^2}{S_n}} \tag{9}$$

To investigate the impact of varying controller gains on the model performance, the dynamic model of the grid-forming control system is simulated with different droop gain values. Figures 6 and 7 show the effect of various lag time constants of the designed controller, i.e., $k_{pd}$ and $k_{qd}$ of the frequency-watt

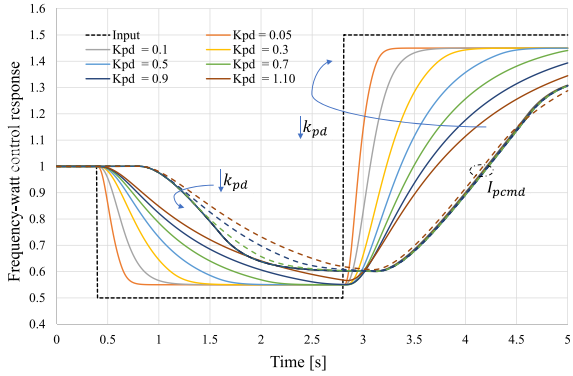


Fig. 6. Traces of frequency-watt response of the grid-forming control system to the step function input.

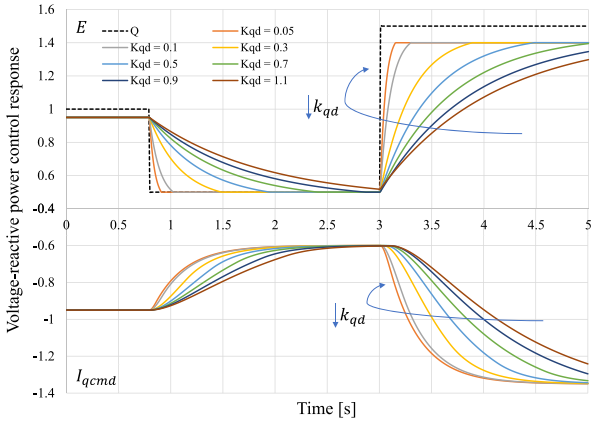


Fig. 7. Traces of voltage-VAR response of the grid-forming control system to the step function input.

and voltage-VAR response from the grid-forming control, respectively. To assess the model's performance, a step function input was applied to study the effect of an active power change on the frequency and reactive power when providing the voltage support service. For example, the system input is decreased to 0.5 at time $t = 0.4$ second, and then increased to

TABLE I
PARAMETER VALUES FOR THE PROPOSED DROOP-BASED CONTROLLER

| Parameter | Value | Parameter description |
|---|---|---|
| $dbd1$ | -0.05 | Lower voltage deadband |
| $dbd2$ | 0.05 | Upper voltage deadband |
| $k_{qv}$ | 8 | Proportional voltage control gain |
| $P_{max}$ | 1.2 | Maximum active power |
| $P_{min}$ | 0 | Minimum active power |
| $dP_{up}$ | 0.5 | Power ramp-up rate |
| $dP_{down}$ | -0.5 | Power ramp-down rate |
| $T_{pord}$ | 0.04 | Power order time constant |
| $I_{max}$ | 1.35 | Maximum converter current |
| $T_g$ | 0.04 | Time constant in the current controller |
| $rrpwr$ | 0.5 | Power rise ramp rate following a fault |
| $I_{qh1}$ | 1.1 | Maximum of reactive current boost injection |
| $I_{ql1}$ | -1.1 | Minimum of reactive current boost injection |

1.5 at time $t = 2.8$ second. In both cases, the system response is evident, although the reaction time varies depending on the set points of the controller gain. Furthermore, the impacts of the droop gain parameter on $I_{pcmd}$ and $I_{qcmd}$ in the output of the current limiter control section are shown in Figs. 6 and 7, respectively. The current control effectively limits inrush currents to an acceptable range. Combining a current limiter with a grid-forming control has been shown to enable an inverter system to work as a voltage source, when the current control behavior is near the current limit such as under the black start condition. When the values of $K_{pd}$ and $K_{qd}$ are low, the droop curve of the system has a shallow slope. As a result, the output of the controller is able to follow the input quickly.

The time constant $k_{pd}$ is set according to the acceleration time of the grid. Hence, it is a measure of the inertia contribution of the grid-forming unit, which is proportional to its nominal capacity. The droop parameters $k_p$ and $k_q$ refer to the maximum frequency and voltage drop at the nominal power, respectively. The remaining control parameter values are summarized in Table I.

*2) Stability Improvement of the Weak Grid by SPS:* In this scenario, it is assumed that all onshore loads will be supplied by the sole generator at Bus 1, as indicated by the red trajectory in Fig. 4. To emulate a weak grid, the generator dispatch is gradually reduced to its minimum capacity over time and eventually taken out of service. The integrated dynamic simulation is performed by importing the SPS model to PSS/Netomac, and then both grids and the DC-link simulation are analyzed in the PSS/Netomac workspace. State space equations for stability analysis for grid-forming inverters are detailed in [33]. Within the 10 s simulation time frame, the generator dispatch level is intentionally reduced to its minimum capacity at $t = 4$ s, and then it is taken out of service at $t = 4.4$ s. It is observed from the simulated voltage profile in Fig. 8(a) that, the system becomes unstable immediately after the blackout. However, the SPS interconnection through grid-forming control helps the system to return to a stable state shortly after displaying the transient behavior. It is observed from the frequency profile in Fig. 8(b) that, there is

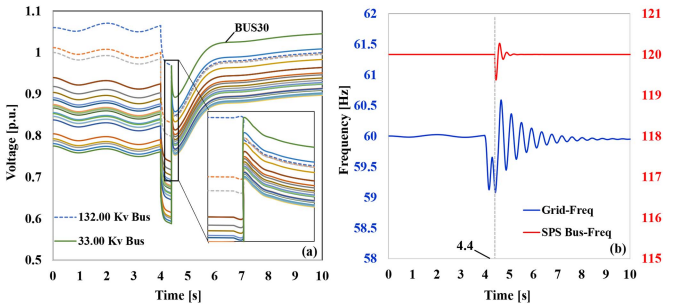


Fig. 8. (a) System voltage and (b) frequency profiles for the interconnected SPS to the onshore grid.

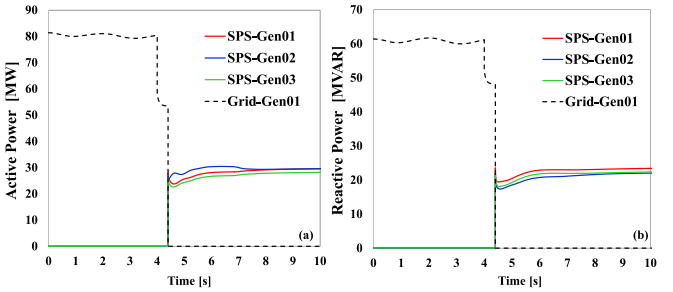


Fig. 9. (a) Active and (b) reactive power sharing of the generators in the interconnected SPS to the onshore grid.

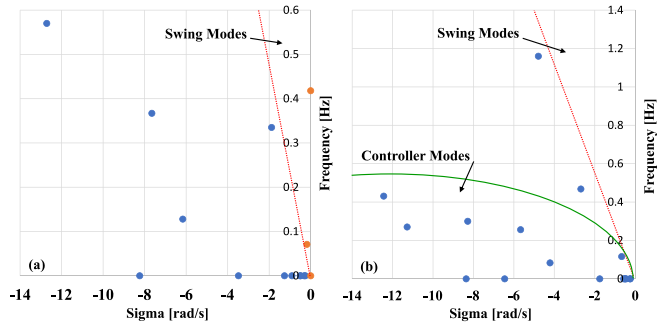


Fig. 10. System eigenvalue trajectory: (a) Coastline power grid without SPS; (b) SPS interconnected to the onshore grid.

a frequency drop in the bus on the SPS side at the moment of interconnection. However, this disturbance does not propagate to the rest of the system due to the isolation provided by the DC-link.

The active and reactive power output profiles of Bus 1 and SPS generators are illustrated in Fig. 9. To prevent instability in the grid, the sole generator at Bus 1 is taken out of service when the SPS is connected to the grid. In addition to time-domain simulation results, an extensive eigenvalue analysis has been conducted to study the impact of the designed controller on dynamic performance and stability of the whole system, and the results are shown in Fig. 10. Figure 10(a) shows the eigenvalue profile without connecting SPS to the coastline grid. Because the poles are located in the swing zone, the system is operating in the swing mode of operation, due to the presence of eigenvalues in the swing region (swing modes lie near the imaginary axis on the complex S-plane in the range of 0.5 to 18, corresponding to the oscillation

frequency ranging from 0.1 to 3 Hz). Hence, the system shows a fluctuating response in time domain simulations with this configuration.

However, after the interconnection of the SPS to the coastline grid, most of the controller modes are seen to be located in the controller region as displayed in Fig. 10(b). These modes are monotonous modes with strong damping capacity, generally associated with first-order delay elements of small time constants. For a safe operation of a power system, it is required that all modes are stable. Moreover, all the oscillation modes should be damped out as quickly as possible. In this study, all existing modes are set to have at least a 10% damping ratio which further verifies the accuracy of the simulation.

*3) Black Start Process of the Coastline Grid by SPS:* In this scenario, the hurricane is assumed to traverse the grid along trajectory 2 (blue line) as shown in Fig. 4. As a result, there are no generators available in the onshore grid to supply power. The grid-forming control scheme creates the voltage and frequency reference for the integrated system. To initiate the black start process, the two transformers which are connected to Bus-30 (33 kV) & Bus-4 (132 kV) are first energized by SPS, for creating the voltage and frequency reference. It is seen from Figs. 11(a) and (b) that, during the initial two seconds of simulations, the coastal grid experiences no load and grid-forming support is solely utilized for voltage and frequency stabilization during the transformer energization period. To regulate the inrush current during black start, transformers are progressively activated on land in a sequence, with their control systems meticulously synchronized to initiate them gradually over time. This method helps to prevent a sudden surge in inrush current. The grid was partitioned into three zones, and only one zone was energized at each stage until the entire grid was restored. Therefore, at $t = 2$ s, the load at Bus-30 and Bus-4 is connected to the grid. At $t = 3$ s, the lines between Bus(30-29) and Bus(30-27) are closed and Zone 1 is energized. The result in voltage dip is found to be approximately 8%. At $t = 7$ s, Zone 2 is restored, and finally, at $t = 11$ s, Zone 3 is picked up. Once Zone 3 is energized, the grid will recover completely from the blackout. The system encounters the highest loading at $t = 11$ s when Zone 3 (+40 MW loading) is connected. It leads to a momentary voltage drop as displayed in Fig. 11(a).

It is observed from the transient frequency profile in Fig. 11(b) that, the sudden loading from Zone 2 at $t = 7$ s results in a frequency drop of approximately 0.82 Hz, which is the lowest frequency nadir in the whole re-energization process. In the *d* current control mode of the current controller, the significance of voltage in the black start process results in the controller ramping up voltage references, by controlling reactive power and regulating the *q* component of the current in the voltage loop. Subsequently, the controller increases the *d* component of the current to inject active power into the grid, while also regulating the voltage and frequency of the inverter system to ensure synchronization with the grid. According to Fig. 11, the energization of Zone 2 causes a voltage drop at the PCC. The power flow direction changes and the system settles down at a new voltage set-point. During the sequential grid energization process, the frequency profile reflects

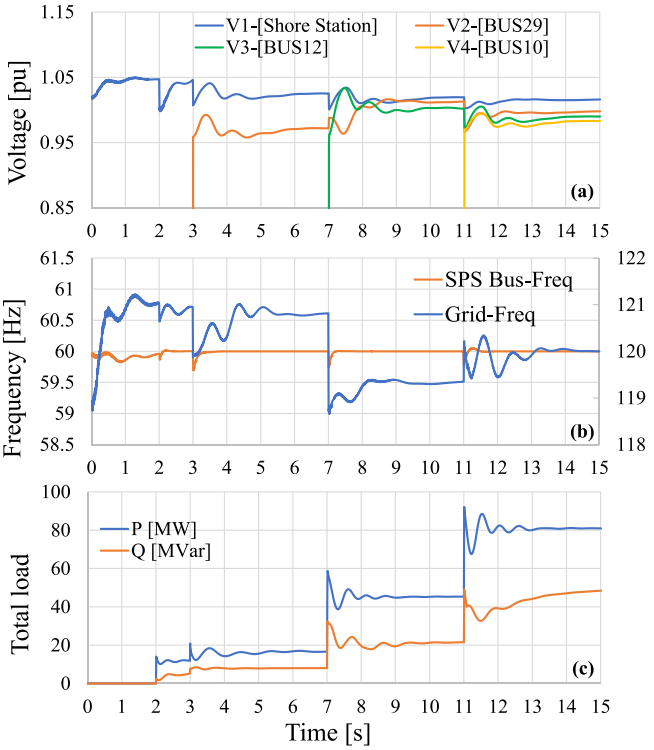


Fig. 11. Dynamic simulation results of the black start of the grid with SPS: (a) voltage amplitude of the buses, (b) grid and SPS frequency profiles, and (c) total active and reactive load pick up.

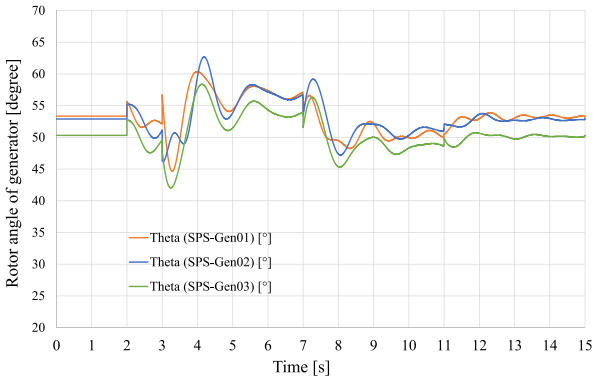


Fig. 12. The rotor angle profile of all the generators in the SPS system during the black start.

the changing loading level of the system. The SPS operates at 120 Hz and the grid operates at 60 Hz. Figure 11(b) depicts the transient frequency in both the terrestrial and SPS grids. The red line represents the SPS frequency profile during the black start. The grid-forming DC-link successfully maintains the SPS frequency, without causing a lot of fluctuations during the load pick-up events. The frequency is only observed to drop at the sudden loading moments. The dynamic rotor angle profile (i.e., one of the prime stability measures) is found to be residing within normal operating limits, thus validating the effectiveness and capability of the proposed grid-forming control. As shown in Fig. 12, the rotor angles of the generator units inside the SPS remain within normal operating conditions throughout the simulation, and the system can maintain

reasonable performance by increasing the load to the nominal value of the generators.

## V. Conclusion

This study investigated the utilization of shipboard power system (SPS) to enhance the resilience of the power grid during disruptive events, such as blackouts. Specifically, the potential of ship-to-grid integration for black start of a coastline grid was evaluated. Due to the differences in power system characteristics, such as voltage and frequency profiles, between the SPS and shoreline grid, a DC-link scheme was proposed for ship-to-grid connection. A grid-forming control scheme was developed to provide a stable voltage and frequency reference, which is essential for initiating the black start process. Additionally, current limit controller units were included to model the inverter as a voltage source in support of the grid. All the controllers pertaining to the grid-forming control scheme, including the droop controller, current limiter, and grid interface of the DC-link, were modeled in PSS/Netomac. Furthermore, the dynamic simulation of the energization process showed that the grid-forming DC-link control scheme was capable of providing the black start service while maintaining the stability of both the coastline power grid and the SPS. The study can make a valuable contribution to the development of new technologies and methodologies for enhancing the resilience and reliability of power systems in the face of blackouts and other disturbances.

Potential future work could explore the impact of onboard battery packs in electrical ships and determine the optimal fleet size of electrical ships to improve the stability and resilience of the coastline power grid through grid-forming support services.

## Acknowledgment

The United States Government has a royalty-free license throughout the world in all copyrightable material contained herein. Any opinions, findings, and conclusions or recommendations expressed in this material are those of the author(s) and do not necessarily reflect the views of the Office of Naval Research and Department of Energy.

## References

[1] A. B. SMITH. "2020 U.S. billion-dollar weather and climate disasters in historical context." Sep. 27, 2021. [Online]. Available: https://www.climate.gov/disasters2020

[2] J. Xue, F. Mohammadi, X. Li, M. Sahraei-Ardakani, G. Ou, and Z. Pu, "Impact of transmission tower-line interaction to the bulk power system during hurricane," *Rel. Eng. Syst. Safety*, vol. 203, Nov. 2020, Art. no. 107079.

[3] Z. Li, M. Shahidehpour, F. Aminifar, A. Alabdulwahab, and Y. Al-Turki, "Networked microgrids for enhancing the power system resilience," *Proc. IEEE*, vol. 105, no. 7, pp. 1289–1310, Jul. 2017.

[4] H. Zhang, P. Wang, S. Yao, X. Liu, and T. Zhao, "Resilience assessment of interdependent energy systems under hurricanes," *IEEE Trans. Power Syst.*, vol. 35, no. 5, pp. 3682–3694, Sep. 2020.

[5] E. B. Watson and A. H. Etemadi, "Modeling electrical grid resilience under hurricane wind conditions with increased solar and wind power generation," *IEEE Trans. Power Syst.*, vol. 35, no. 2, pp. 929–937, Mar. 2020.

[6] L. Che and M. Shahidehpour, "Adaptive formation of Microgrids with mobile emergency resources for critical service restoration in extreme conditions," *IEEE Trans. Power Syst.*, vol. 34, no. 1, pp. 742–753, Jan. 2019.

[7] A. Vlachokostas et al., "Ship-to-grid integration: Environmental mitigation and critical infrastructure resilience," in *Proc. IEEE Elect. Ship Technol. Symp. (ESTS)*, 2019, pp. 542–547.

[8] A. Spinosa, A. Ziemba, A. Saponieri, L. Damiani, and G. El Serafy, "Remote sensing-based automatic detection of shoreline position: A case study in Apulia region," *J. Mar. Sci. Eng.*, vol. 9, no. 6, p. 575, 2021.

[9] S. Rahman and I. A. Khan, "Investigation of power quality issues in cold ironed (shore connected) grid connected electric ships," in *Proc. 54th Asilomar Conf. Signals Syst. Comput.*, 2020, pp. 1353–1358.

[10] S. Karimi, M. Zadeh, and J. A. Suul, "A Multilayer framework for reliability assessment of shore-to-ship fast charging system design," *IEEE Trans. Transport. Electrific.*, vol. 8, no. 3, pp. 3028–3040, Sep. 2022.

[11] M. Dabbaghjamanesh, S. Senemmar, and J. Zhang, "Resilient distribution networks considering mobile marine Microgrids: A synergistic network approach," *IEEE Trans. Ind. Informat.*, vol. 17, no. 8, pp. 5742–5750, Aug. 2021.

[12] S. Wen et al., "Coordinated optimal energy management and voyage scheduling for all-electric ships based on predicted shore-side electricity price," *IEEE Trans. Ind. Appl.*, vol. 57, no. 1, pp. 139–148, Jan./Feb. 2021.

[13] D. Zhou, C. Wu, Q. Sui, X. Lin, and Z. Li, "A novel all-electric-ship-integrated energy cooperation coalition for multi-island microgrids," *Appl. Energy*, vol. 320, Aug. 2022, Art. no. 119280.

[14] A. Vicenzutti, F. Tosato, G. Sulligoi, G. Lipardi, and L. Piva, "High voltage ship-to-shore connection for electric power supply support in landing operations: An analysis," in *Proc. IEEE Elect. Ship Technol. Symp. (ESTS)*, 2015, pp. 364–369.

[15] G. Guidi, J. A. Suul, F. Jenset, and I. Sorfonn, "Wireless charging for ships: High-power inductive charging for battery electric and plug-in hybrid vessels," *IEEE Electrific. Mag.*, vol. 5, no. 3, pp. 22–32, Sep. 2017.

[16] S. Badakhshan, S. Senemmar, and J. Zhang, "Dynamic feasibility assessment of ship-to-grid interconnection by DC-link," in *Proc. IEEE Texas Power Energy Conf. (TPEC)*, 2022, pp. 1–6.

[17] L. F. N. Lourenço, F. Perez, A. Iovine, G. Damm, R. M. Monaro, and M. B. C. Salles, "Stability analysis of grid-forming MMC-HVDC transmission connected to legacy power systems," *Energies*, vol. 14, no. 23, p. 8017, 2021.

[18] I. Ray and L. M. Tolbert, "Grid-forming inverter control design for PV sources considering DC-link dynamics," *IET Renew. Power Gener.*, Mar. 2022, doi: 10.1049/rpg2.12454.

[19] E. Rokrok, T. Qoria, A. Bruyere, B. Francois, and X. Guillaud, "Classification and dynamic assessment of droop-based grid-forming control schemes: Application in HVDC systems," *Elect. Power Syst. Res.*, vol. 189, Dec. 2020, Art. no. 106765.

[20] Z. Zhang, Y. Jin, and Z. Xu, "Grid-forming control of wind turbines for diode rectifier unit based offshore wind farm integration," *IEEE Trans. Power Del.*, vol. 38, no. 2, pp. 1341–1352, Apr. 2023.

[21] W. Du et al., "A comparative study of two widely used grid-forming droop controls on Microgrid small-signal stability," *IEEE J. Emerg. Sel. Topics Power Electron.*, vol. 8, no. 2, pp. 963–975, Jun. 2020.

[22] M. Li et al., "Unified modeling and analysis of dynamic power coupling for grid-forming converters," *IEEE Trans. Power Electron.*, vol. 37, no. 2, pp. 2321–2337, Feb. 2022.

[23] F. Zhao, X. Wang, and T. Zhu, "Power dynamic decoupling control of grid-forming converter in stiff grid," *IEEE Trans. Power Electron.*, vol. 37, no. 8, pp. 9073–9088, Aug. 2022.

[24] E. Team. "Model description document: Notional four zone MVDC shipboard power system model." 2020. [Online]. Available: www.esrdc.com

[25] G. Sulligoi, D. Bosich, R. Pelaschiar, G. Lipardi, and F. Tosato, "Shore-to-ship power," *Proc. IEEE*, vol. 103, no. 12, pp. 2381–2400, Dec. 2015.

[26] M. Chen, D. Zhou, A. Tayyebi, E. Prieto-Araujo, F. Dörfler, and F. Blaabjerg, "Generalized Multivariable grid-forming control design for power converters," *IEEE Trans. Smart Grid*, vol. 13, no. 4, pp. 2873–2885, Jul. 2022.

[27] J. M. Guerrero, J. C. Vasquez, J. Matas, M. Castilla, and L. Garcia de Vicuna, "Control strategy for flexible Microgrid based on parallel line-interactive UPS systems," *IEEE Trans. Ind. Electron.*, vol. 56, no. 3, pp. 726–736, Mar. 2009.

[28] T. Chen, Y. Song, D. J. Hill, and A. Y. S. Lam, "Chance-constrained OPF in droop-controlled Microgrids with power flow routers," *IEEE Trans. Smart Grid*, vol. 13, no. 4, pp. 2601–2613, Jul. 2022.

[29] E. Rokrok, T. Qoria, A. Bruyere, B. Francois, and X. Guillaud, "Transient stability assessment and enhancement of grid-forming converters embedding current reference saturation as current limiting strategy," *IEEE Trans. Power Syst.*, vol. 37, no. 2, pp. 1519–1531, Mar. 2022.
[30] M. G. Taul, X. Wang, P. Davari, and F. Blaabjerg, "Current limiting control with enhanced dynamics of grid-forming converters during fault conditions," *IEEE J. Emerg. Sel. Topics Power Electron.*, vol. 8, no. 2, pp. 1062–1073, Jun. 2020.
[31] T. Hathiyaldeniye, U. D. Annakkage, N. Pahalawaththa, and C. Karawita, "A comparison of inverter control modes for maintaining voltage stability during system contingencies," *IEEE Open Access J. Power Energy*, vol. 9, pp. 55–65, 2022.
[32] J. Venkateswaran, P. Manohar, K. Vinothini., B. Shree, and R. Jayabarathi, "Contingency analysis of an IEEE 30 bus system," in *Proc. 3rd IEEE Int. Conf. Recent Trends Electron. Inf. & Commun. Technol. (RTEICT)*, 2018, pp. 328–333.
[33] L. Ding et al., "Region-based stability analysis of resilient distribution systems with hybrid grid-forming and grid-following inverters," in *Proc. IEEE Energy Convers. Congr. Expo. (ECCE)*, 2020, pp. 3733–3740.

**Sobhan Badakhshan** (Graduate Student Member, IEEE) received the B.S. degree in electrical engineering from the Iran University of Science and Technology, Tehran, Iran, in 2013, and the M.S. degree in electrical engineering from the Sharif University of Technology, Tehran, in 2015. He is currently pursuing the Ph.D. degree in electrical engineering with The University of Texas at Dallas, Richardson, TX, USA. His research interests focus on enhancing the reliability and resilience of the power system, with a primary emphasis on machine learning-enabled methods, as well as the economic and secure optimization of electric systems with renewable energy integration.

**Jubeyer Rahman** (Graduate Student Member, IEEE) received the B.S. degree in electrical and electronic engineering from the Bangladesh University of Engineering and Technology in 2012, and the M.S. degree in electrical engineering from the University of Hawaii at Manoa, Honolulu, HI, USA, in 2018. He is currently pursuing the Ph.D. degree in electrical engineering with The University of Texas at Dallas, Richardson, TX, USA. His research interests include multi-timescale power system operation, capacity expansion planning of renewable intensive power grid, integrated energy systems, microgrid control, and electricity and energy market.

**Jie Zhang** (Senior Member, IEEE) received the B.S. and M.S. degrees in mechanical engineering from the Huazhong University of Science and Technology, Wuhan, China, in 2006 and 2008, respectively, and the Ph.D. degree in mechanical engineering from Rensselaer Polytechnic Institute, Troy, NY, USA, in 2012. He is currently an Associate Professor with the Department of Mechanical Engineering and the Department of Electrical and Computer Engineering, The University of Texas at Dallas. His research interests include integrated energy systems, renewable energy grid integration, complex networks, machine learning, and multidisciplinary design optimization.